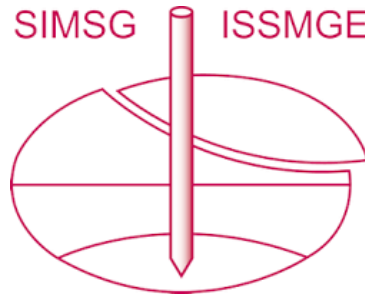


# INTERNATIONAL SOCIETY FOR SOIL MECHANICS AND GEOTECHNICAL ENGINEERING



*This paper was downloaded from the Online Library of the International Society for Soil Mechanics and Geotechnical Engineering (ISSMGE). The library is available here:*

<https://www.issmge.org/publications/online-library>

*This is an open-access database that archives thousands of papers published under the Auspices of the ISSMGE and maintained by the Innovation and Development Committee of ISSMGE.*

*The paper was published in the proceedings of the 10th European Conference on Numerical Methods in Geotechnical Engineering and was edited by Lidija Zdravkovic, Stavroula Kontoe, Aikaterini Tsiampousi and David Taborda. The conference was held from June 26<sup>th</sup> to June 28<sup>th</sup> 2023 at the Imperial College London, United Kingdom.*

*To see the complete list of papers in the proceedings visit the link below:*

<https://issmge.org/files/NUMGE2023-Preface.pdf>

# A review of parameters for hypoplastic constitutive models

Amir Mosallaei<sup>1</sup>, András Mahler<sup>1</sup>

<sup>1</sup> *Department of Engineering Geology and Geotechnics, Budapest University of Technology and Economics, Budapest, HU*

**ABSTRACT:** The soil constitutive equation describes the relationship between stress and strain tensor, which varies based on soil type and deformation conditions. The development of different constitutive models, also known as constitutive relations, has enabled a comprehensive understanding of the macromechanical properties of soil. Over the years, soil mechanics has explored the complex behavior of soils to gain a better understanding of their constitutive relations. This has led to the creation of various models that can help describe and explain the behavior of soil. Hypoplasticity is one such constitutive equation that was discovered over three decades ago. Nonetheless, even if a perfect constitutive model exists, it is of no value until its parameters or constants are known. As a result, it is essential to calibrate material parameters for successful application of constitutive models. Therefore, the purpose of this paper is to review various approaches for determining hypoplasticity parameters for sand and identify an appropriate range for these variables.

**Keywords:** Hypoplasticity; Coarse-grained soil; Intergranular strain; Triaxial test

## 1 INTRODUCTION

The complex domain of constitutive modeling of soils necessitates an in-depth comprehension of soil testing and behavior, advanced mathematics, and abstraction. Constitutive equations are essential in solid mechanics for mathematically describing the mechanical behavior of a material, but they define ideal materials and may only partially represent the actual material. Nevertheless, they provide a mathematical tool for predicting physical system behavior based on limited experimental observations. The finite element method is frequently employed in geotechnical engineering to address design problems, and it invariably necessitates sophisticated constitutive models to realistically represent soil behavior. Even though several advanced models exist, they do not entirely satisfy general conditions and necessitate further research. Hypoplasticity arises from the framework of rational mechanics and is distinguished by its simplicity (Brinkgreve, 2005).

To gain a better comprehension of hypoplasticity, it is preferable to familiarize oneself with other material behaviors, such as elasticity, plasticity, and elastoplasticity. The following is a brief overview of these behaviors.

Elasticity pertains to a material's ability to return to its original stress-free state without energy dissipation and is represented by stress as a function of strain. Hyperelasticity, on the other hand, necessitates an energy potential. Plasticity refers to a type of material behavior in which deformation is dissipative and stress depends on the path of deformation. Elastoplasticity

merges elasticity and plasticity and is the dominant form of constitutive model used. In contrast, hypoplasticity is an alternative to elastoplasticity that utilizes constitutive models that are path-dependent and dissipative without a yield surface. Dissipative behavior is modeled using non-linear rate equations, but if the equation is linear, a non-dissipative model called hypoelasticity is produced.

## 2 HYPOPLASTICITY

The constitutive law used in hypoplasticity is a rate-type, incrementally nonlinear equation based on the concept proposed by Kolymbas (Kolymbas, 1991). Unlike incrementally linear equations for hyperelastic and hypoelastic material laws, the hypoplastic constitutive equations are not differentiable at zero strain rate because of the different stiffnesses for loading and unloading common in inelastic materials (von Wolffersdorff, 1996). The strain in hypoplasticity is not decomposed into elastic and plastic parts, which differs from the classical elastoplastic concept (Bauer et al., 2020).

Most of the fundamental characteristics of soil behavior are encompassed in hypoplasticity, including the relationship between soil stiffness and void ratio and stress level (Kadlíček et al., 2016).

The hypoplastic model can consider the effects of pressure and density, and its parameters can be determined easily from standard laboratory tests. It is successful in describing the behavior of sand, especially for monotonous deformation paths, and even for soft soils with a high critical friction angle. It performs well for

deformations caused by rearrangements of the grain skeleton, but it has some defects when applied to cyclic stressing or deformation with small amplitudes, such as excessive deformation predicted for small stress cycles called ratcheting. A change in direction of the strain path results in an increase in stiffness, and the maximum value appears with a complete strain rate reversal (Niemunis & Herle, 1997).

## 2.1 Basic parameters

To describe the behavior of soil using hypoplasticity, eight fundamental parameters are used. These parameters include critical friction angle ( $\varphi_c$ ), granular hardness ( $h_s$ ), and its exponent ( $n$ ), critical void ratio at zero pressure ( $e_{c0}$ ), maximum void ratio at zero pressure ( $e_{i0}$ ), minimum void ratio at zero pressure ( $e_{d0}$ ), as well as exponents  $\alpha$  and  $\beta$  (Namaei-kohal et al., 2022).

### 2.1.1 Critical state friction angle ( $\varphi_c$ )

Typically, soil under monotonic shear loading reaches its critical state when volumetric deformation rate stabilizes at a certain level while maintaining constant mean stress. To determine critical state, triaxial test is commonly used, but deformation localization into a shear band may affect stress measurements. To minimize this effect, frictionless platens and loose sample preparation are recommended. Measuring the angle of repose can approximate the critical friction angle for soils with grain sizes larger than 0.1mm, while the funnel method is preferred for sand soil. The funnel test involves slowly lifting a funnel filled with soil to create a heap close to critical state. Contact between the funnel and forming heap should be constant and the base beneath the heap should be rough to prevent sliding (Kadlíček et al., 2016).

### 2.1.2 Granular hardness ( $h_s$ ) & Barotropy exponent ( $n$ )

Granular hardness ( $h_s$ ) is the only parameter with the dimension of stress and should not be confused with the hardness of individual grains. The exponent "n" takes into account the pressure-sensitivity of the grain skeleton, allowing for a non-proportional increase in incremental stiffness with increasing pressure. An oedometer test is simpler than isotropic compression for determining  $h_s$  and  $n$ , with a dry or water-saturated specimen used to suppress physico-chemical effects. Obtaining  $h_s$  and  $n$  directly from measured data is not recommended due to strong non-linearity. The knowledge of  $n$  is necessary for determining  $h_s$ , but  $n$  can be calculated independently of  $h_s$ . Oedometer test can replace isotropic compression for calibration as it is easier to perform and allows for reaching higher pressure, as  $h_s$  and  $n$  control the slope and curvature of the compression line, respectively (Herle & Gudehus, 1999; Kadlíček et al., 2016).

### 2.1.3 Minimum ( $e_{d0}$ ), Critical ( $e_{c0}$ ) & Maximum void ratio at zero pressure ( $e_{i0}$ )

To obtain the best densification of granular material, cyclic shearing with small amplitude under constant pressure after static compression can lead to an asymptotic minimum void ratio  $e_{d0}$ , which is slightly lower than but close to  $e_{min}$ . Void ratios  $e_{c0}$ ,  $e_{d0}$ , and  $e_{i0}$  determine the positions of the limiting void ratio curves in  $e$ - $\ln p$  space, with  $e_{c0}$  setting the position of the critical state line,  $e_{d0}$  controlling the position of the minimal void ratio curve, and  $e_{i0}$  representing the maximum void ratio of a grain skeleton reached during isotropic consolidation in a gravity-free space. To determine  $e_{c0}$ , the triaxial test or an oedometer test assuming the soil is in its loosest state can be used. The maximal void ratio  $e_{max}$  can be determined through various laboratory methods and is typically denser than the theoretical maximum. Empirically,  $e_{d0}/e_{max}$  ratios of 1.2 for spheres and 1.3 for cubes have been found (Herle & Gudehus, 1999; Kadlíček et al., 2016).

### 2.1.4 Dilatancy ( $\alpha$ ) and Pyknotropy exponent ( $\beta$ )

The parameters  $\alpha$  and  $\beta$ , which govern the development of stiffness and pyknotropy factors, need to be evaluated using a parametric study that involves simulating the triaxial shear test and depends on knowledge of the preceding parameters. In the case of natural sands, it is generally sufficient to assume  $\beta = 1$ , regardless of granulometric properties (Herle & Gudehus, 1999; Kadlíček et al., 2016).

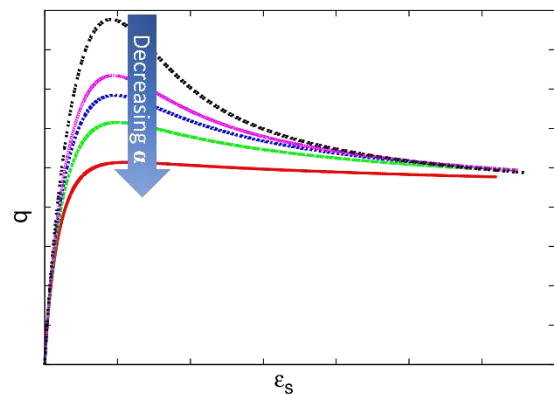


Figure 1. Effect of  $\alpha$  on the peak of stress-strain curve

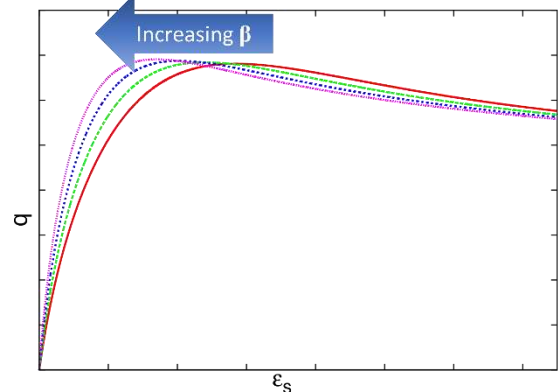


Figure 2. Effect of  $\beta$  on the peak of stress-strain curve

The impact of  $\alpha$  and  $\beta$  parameters on stress-strain curves can be understood through Figure 1 and Figure 2. A drained triaxial test on a dense sample and curve simulation using various amounts of  $\alpha$  can be conducted to calibrate these parameters. Fitting the resulting curves will yield the optimal value for  $\alpha$ . Figure 1 shows that increasing  $\alpha$  decreases the stress peak on the stress-strain curve, while  $\beta$  changes the location of the peak by reducing the strain value and shifting the peak to the left.

To calibrate a set of hypoplasticity parameters, the following minimum laboratory measurements are required. The parameters can be divided into three categories. The first category is critical friction angle ( $\varphi_c$ ),

which can be calibrated using an angle of repose test performed with a funnel. The second category includes granular hardness ( $h_s$ ), exponent ( $n$ ), minimum void ratio at zero pressure ( $e_{d0}$ ), and maximum void ratio at zero pressure ( $e_{i0}$ ), which can be calibrated using an oedometer test on a soil at its loosest possible state. Critical void ratio at zero pressure ( $e_{c0}$ ) can also be classified in this category and obtained using the empirical formula  $e_{d0}=0.5*e_{c0}$ . The third and final category involves parameters  $\alpha$  and  $\beta$ , which can be calibrated using a drained triaxial test on densely compacted soil through a trial-and-error procedure.

Table 1. Hypoplastic parameters of different types of soil

		$\varphi_c$ (°)	$h_s$ (MPa)	$n$	$e_{d0}$	$e_{c0}$	$e_{i0}$	$\alpha$	$\beta$
1	Hochstetten gravel (Brinkgreve, 2005)	36	3.2000E+04	0.18	0.26	0.45	0.5	0.1	1.9
2	Hochstetten sand (Brinkgreve, 2005)	33	1.5000E+03	0.28	0.55	0.95	1.05	0.25	1
3	Hostun sand (Brinkgreve, 2005)	31	1.0000E+03	0.29	0.61	0.96	1.09	0.13	2
4	Karlsruhe sand (Mašín, 2019)	30	5.8000E+03	0.28	0.53	0.84	1	0.13	1
5	Lausitz sand (Herle & Gudehus, 1999)	33	1.6000E+03	0.19	0.44	0.85	1	0.25	1
6	Toyoura sand(Herle & Gudehus, 1999)	30	2.6000E+03	0.27	0.61	0.98	1.1	0.18	1.1
7	Zbraslav sand(Herle & Gudehus, 1999)	31	5.7000E+03	0.25	0.52	0.82	0.95	0.13	1
8	Uncemented gravel (Fu et al., 2021)	39.5	7.5000E+01	0.55	0.17	0.40	0.48	0.06	1.5
9	Uncemented sand (Fu et al., 2021)	28.6	9.5500E+01	0.45	0.48	0.75	0.86	0.15	1.25
10	Karlsruhe fine sand (Poblete et al., 2016)	33	8.6260E+01	0.32	0.67	1.09	1.21	0.21	1.5
11	Karlsruhe fine sand (Fuentes et al., 2020)	32.6	4.0000E+03	0.27	0.677	1.054	1.212	0.14	2.5
12	Prague sand (Kadlíček et al., 2016)	35.47	9.0530E+01	0.56	0.33	0.66	0.79	0.03	1.9
13	Komorany sand (Mašín, 2019)	35	5.0000E+01	0.2	0.35	0.87	1.04	0.26	4
14	Dobransy (Kadlíček et al., 2022)	41.1	6.5339E+01	0.207	0.592	1.183	1.42	0.05	4
15	Hrusovany (Kadlíček et al., 2022)	42.6	1.9030E+00	0.162	0.591	1.182	1.418	0.07	6.3
16	Jablonec (Kadlíček et al., 2022)	42.6	1.0370E+00	0.232	0.616	1.232	1.478	0.02	4.1
17	Kralupy (Kadlíček et al., 2022)	41.2	1.7560E+00	0.149	0.809	1.1618	1.942	0.23	4.8
18	Stvanice (Kadlíček et al., 2022)	35.8	8.5300E-01	0.199	0.844	1.689	2.026	0.23	4.9
19	Hochstetten sand (Khalaj et al., 2021)	33	1.5000E+03	0.28	0.55	0.95	1.05	0.25	1.5
20	Toyoura sand (Ng et al., 2013)	30	2.6000E+03	0.27	0.61	0.98	1.1	0.14	3
21	Firoozkuh sand (Mohammadi-Haji & Ardakani, 2020)	32.7	3.5000E+02	0.24	0.58	0.91	1.1	0.5	1
22	Hostun sand (Moussa et al., 2020)	32	1.0000E+03	0.29	0.61	0.96	1.09	0.13	2
23	Tehran silica sand (Namaei-kohal et al., 2022)	38.4	4.6000E+02	0.26	0.41	0.82	0.98	0.3	1.5
24	Hochstetten sand (Niemunis & Herle, 1997)	33	1.0000E+03	0.25	0.55	0.95	1.05	0.25	-
25	Used for model (Niemunis et al., 2005)	32.8	1.5000E+02	0.4	0.575	0.908	1.044	0.12	1
26	Original model (Yang et al., 2020)	34	3.6000E+03	0.43	0.72	0.934	1.2	0.24	1.2
27	Karlsruhe sand (H. Stutz et al., 2017)	31	1.0000E+03	0.29	0.61	0.96	1.09	0.13	2
28	Toyoura sand (H. Stutz et al., 2016)	30	2.6000E+03	0.27	0.61	0.98	1.1	0.25	1
29	Ticino sand (H. Stutz et al., 2016)	31	1.0000E+03	0.29	0.61	0.96	1.09	0.13	2
30	Density sand (H. Stutz et al., 2016)	32	7.5000E+02	0.25	0.62	0.97	1.06	0.13	1.5
31	Toyura sand (H. H. Stutz & Wuttke, 2018)	31	1.0000E+03	0.29	0.61	0.96	1.09	0.13	2
32	Sandy silt (Tasan & Yilmaz, 2019)	31.5	2.3000E+03	0.30	0.391	0.688	0.791	0.13	1
33	Castro sand (Tsegaye et al., 2010)	30.5	1.1070E+03	0.26	0.5	0.8	0.97	0.2	2
34	Karlsruhe fine sand (Wichtmann et al., 2019)	33.1	4.0000E+03	0.27	0.677	1.054	1.212	0.14	2.5
35	Kolny sand (Mašín, 2015)	35	4.8000E+02	0.26	0.33	0.87	1.04	0.06	1.47
36	Kolny sand (Mašín, 2019)	36	1.2000E+02	0.49	0.28	0.74	0.89	0.03	1.41

Table 1 lists 36 calibrated sets of basic hypoplastic parameters for various types of coarse-grained soil. The table indicates that each parameter falls within a specific range which is mentioned in the conclusion section.

## 2.2 Intergranular strain

The basic hypoplastic models are inadequate in predicting high initial stiffness and ratcheting, which is the accumulation of strains in stress cycles and stresses in strain cycles. The intergranular strain concept is the most widely used approach to overcome this limitation. The ISA theory provides a useful mathematical platform for developing constitutive models to simulate cyclic loading in soils by considering the effect of recent strain history. The intergranular strain evolution equation is elasto-plastic and based on a simple bounding surface approach. The concept assumes that reversible deformation of the intergranular strain layer, combined with elastic deformation of the grains, accounts for all measured soil deformation at the beginning of the loading process until a certain amount of strain is reached and grains start to rearrange. This reversible deformation is described by an additional component of the model, while the deformation associated with grain rearrangement is irreversible and predicted by the standard hypoplastic model. Introducing the intergranular strain adds five more parameters to the basic parameters, namely  $m_R$ ,  $m_T$ ,  $\beta_r$ ,  $R$ , and  $\chi$ , which are discussed in detail in the following sections (Fuentes et al., 2017; Mašin, 2019; Namaei-kohal et al., 2022).

### 2.2.1 Stiffness factor ( $m_R$ )

The parameter called  $m_R$  is responsible for controlling the strength of the shear modulus at very small strain values, both during initial loading and when the strain path direction is reversed by 180 degrees. The most accurate way to determine the value of  $m_R$  is through shear wave propagation experiments, such as bender element tests. However, it is also possible to measure the shear modulus using static shear tests, although this method is less reliable as it relies on local measurements of sample deformation and strain transducers have a limit of accuracy (Mašin, 2019).

### 2.2.2 Parameter $m_T$

Determining the value of parameter  $m_T$  (or ratio  $m_{rat} = m_T / m_R$ ) through experimentation is challenging. The  $m_{rat}$  value is equivalent to the ratio of initial shear stiffness after a 90-degree change in strain path direction ( $G_{90}$ ) to the initial stiffness ( $G_0$ ), expressed as  $G_{90}/G_0$ .  $G_{90}$  cannot be measured through wave propagation techniques and requires accurate measurements using local strain transducers. However, if such experiments are not feasible for a particular soil, a "standard" value of  $m_{rat}$  is recommended. A default value of 0.7 is

commonly used for  $m_{rat}$  if there is no experimental data available for the soil of interest (Mašin, 2019).

### 2.2.3 Elastic strain amplitude, Intergranular strain hardening parameter and exponent

The intergranular strain concept model uses three parameters:  $R$ ,  $\beta_r$ , and  $\chi$ , each having a unique physical meaning.  $R$  defines the elastic range size in the strain space,  $\beta_r$  controls the intergranular strain tensor's rate of evolution, and  $\chi$  governs the interpolation between the reversible elastic and nonlinear hypoplastic response. Despite their different meanings, these parameters collectively control the stiffness degradation rate with increasing strain, affecting the model predictions. Typically, calibration of these parameters involves triaxial shear experiments with local measurements of deformation to obtain shear modulus versus shear strain curves. An increase in  $R$  is equivalent to a decrease in  $\beta_r$ , and they control the horizontal position of the stiffness degradation curve within the  $G$  versus  $\ln \epsilon_s$  diagram. In contrast,  $\chi$  controls the rate of stiffness decrease with strain, and a higher value of  $\chi$  results in a larger quasi-elastic range size and a faster subsequent rate of stiffness decrease. The calibration of parameter  $\chi$  requires a trial-and-error procedure to fit the experimental data (Mašin, 2019).

Table 2. Intergranular strain parameters of different types of soil

	$m_R$	$m_T$	$R$	$\beta_r$	$\chi$
Hochstetten sand (Niemunis & Herle, 1997)	5	2	1	0.5	6
Karlsruhe sand (Mašin, 2019)	6	3.5	1	0.2	6
Komorany sand (Mašin, 2019)	3.4	1.7	2	0.12	0.7
Toyoura sand (Ng et al., 2013)	8	4	0.2	0.1	1
Firoozkuh (Mohammadi-Haji & Ardakani, 2020)	5	2	1	0.5	3
Tehran silica sand (Namaei-kohal et al., 2022)	3.5	1.5	0.7	0.7	0.8
Used for model (Niemunis et al., 2005)	6.5	3	1	0.1	6
Karlsruhe fine sand (Poblete et al., 2016)	5	3.5	1.4	0.35	7
Sandy silt (Tasan & Yilmaz, 2019)	4.4	2.2	1	0.2	6
Karlsruhe fine sand (Wichtmann et al., 2019)	2.2	1.1	1	0.1	5.5

Table 2 presents various sets of intergranular strain parameters for different types of coarse-grained soil. A range can be established for each parameter, which is specified in the conclusion section.

### 3 DISCUSSION

Table 1 lists different basic parameter sets. Plotting these values on a graph of  $e_{c0}$  versus  $e_{d0}$  (with a dot for each set) yields Figure 3, which has a trendline with a slope of approximately 0.58. This slope can be used to estimate  $e_{d0}$  when its value is unknown. As the value relies on prior studies and appears to align with a previously established empirical formula, it is important to verify whether earlier researchers utilized the same formula or opted for a different methodology. If they indeed used the same formula, it follows that correlation will also match the previous findings, since the graph is based on their data.

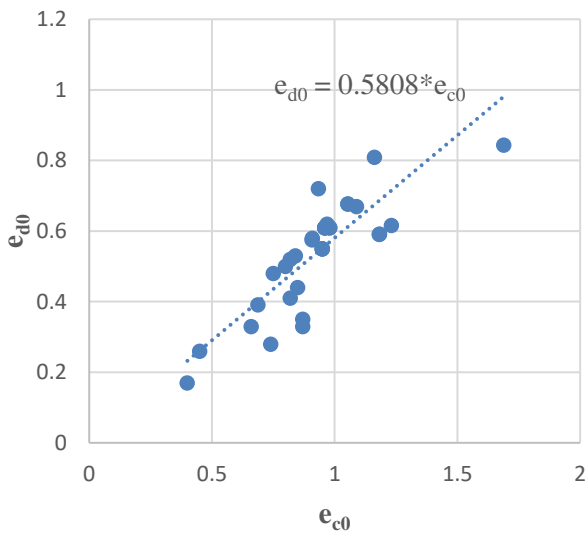


Figure 3. Relation between critical void ratio and minimum void ratio at zero pressure

Previous studies suggest using  $1.2 * e_{c0}$  for spherical grain shapes and  $1.3 * e_{c0}$  for cube grain shapes instead of  $e_{i0}$ . Plotting dots for each set of  $e_{c0}$  and  $e_{i0}$  (according to Table 1) on a graph results in Figure 4, which shows that in most cases, the marked dots are below the empirical formula. The trendline has a slope that indicates  $e_{i0} = 1.18 * e_{c0}$ . As exact values for maximum void ratio are difficult to obtain, the empirical formula can be used to estimate it, with a slightly lower value than previously thought.

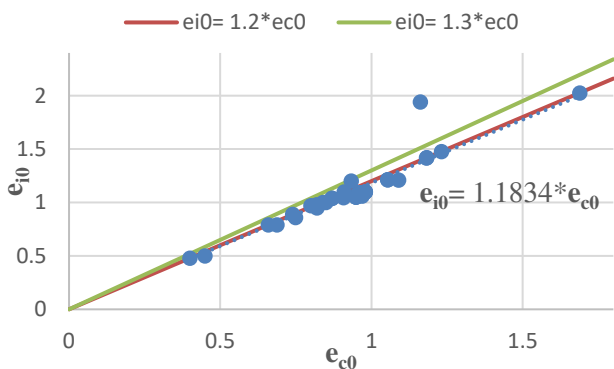


Figure 4. Finding maximum void ratio at zero pressure using empirical formula

Figure 5 shows the relationship between  $m_R$  and  $m_T$ , based on the values in Table 2. Previous studies assumed  $m_T = 0.7 * m_R$ , but this review suggests modifying this to  $m_T = 0.5 * m_R$ .

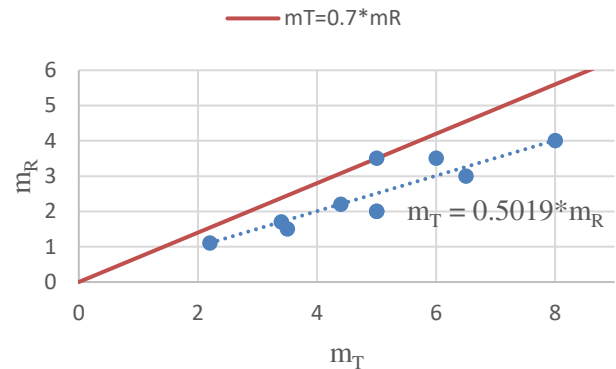


Figure 5. relation between  $m_T$  and  $m_R$

### 4 CONCLUSIONS

The importance of knowing the material parameters in constitutive models for soil behavior cannot be overstated, even if the model itself is perfect. Calibration of these parameters is necessary for successful application of the model. To calibrate the hypoplastic parameters, undrained triaxial, oedometric compression, and drained triaxial tests can be used. Cyclic triaxial testing is necessary to calibrate intergranular strain parameters, but some parameters can be obtained using empirical formulas. This review suggests modifying the empirical formula  $m_T = 0.7 * m_R$  to  $m_T = 0.5 * m_R$ , and provides values for maximum and minimum void ratio at zero pressure ( $1.18 * e_{c0}$  and  $0.58 * e_{c0}$ , respectively). Table 3 presents the defined range for each parameter.

Table 3. An approximate range of parameters

Parameters	Minimum	Maximum
$\varphi_c$ (°)	28.6	42.6
$h_s$ (MPa)	0.853	32000
$n$	0.149	0.56
$e_{d0}$	0.17	0.844
$e_{c0}$	0.4	1.689
$e_{i0}$	0.48	2.026
$\alpha$	0.02	0.5
$\beta$	1	6.3
$m_R$	2.2	8
$m_T$	1.1	4
$R$	0.2	2
$\beta_r$	0.1	0.7
$\chi$	0.7	7

### 5 REFERENCES

Bauer, E., Kovtunen, V. A., Krejčí, P., Krenn, N., Siváková, L., & Zubkova, A. V. (2020). On proportional deformation

- paths in hypoplasticity. *Acta Mechanica*, 231(4), 1603–1619. <https://doi.org/10.1007/s00707-019-02597-3>
- Brinkgreve, R. B. J. (2005). Copyright ASCE 2005 69 Soil Constitutive Models Evaluation, Selection, and Calibration. *Geo-Frontiers Congress 2005*, 69–98.
- Fu, Z., Chen, S., Zhong, Q., & Ji, E. (2021). A damage hypoplasticity constitutive model for cemented sand and gravel materials. *Acta Geotechnica*, 9. <https://doi.org/10.1007/s11440-021-01206-9>
- Fuentes, W., Triantafyllidis, T., & Lascarro, C. (2017). Evaluating the performance of an ISA-hypoplasticity constitutive model on problems with repetitive loading. *Lecture Notes in Applied and Computational Mechanics*, 82, 341–362. [https://doi.org/10.1007/978-3-319-52590-7\\_16](https://doi.org/10.1007/978-3-319-52590-7_16)
- Fuentes, W., Wichtmann, T., Gil, M., & Lascarro, C. (2020). ISA-Hypoplasticity accounting for cyclic mobility effects for liquefaction analysis. *Acta Geotechnica*, 15(6), 1513–1531. <https://doi.org/10.1007/s11440-019-00846-2>
- Herle, I., & Gudehus, G. (1999). Determination of parameters of a hypoplastic constitutive model from properties of grain assemblies. *Mechanics of Cohesive-Frictional Materials*, 4(5), 461–486. [https://doi.org/10.1002/\(SICI\)1099-1484\(199909\)4:5<461::AID-CFM71>3.0.CO;2-P](https://doi.org/10.1002/(SICI)1099-1484(199909)4:5<461::AID-CFM71>3.0.CO;2-P)
- Kadlíček, T., Janda, T., & Šejnoha, M. (2016). Calibration of Hypoplastic Models for Soils. *Applied Mechanics and Materials*, 821, 503–511. <https://doi.org/10.4028/www.scientific.net/amm.821.503>
- Kadlíček, T., Janda, T., Šejnoha, M., Mašín, D., Najser, J., & Beneš, Š. (2022). Automated calibration of advanced soil constitutive models. Part I: hypoplastic sand. *Acta Geotechnica*, 17(8), 3421–3438. <https://doi.org/10.1007/s11440-021-01441-0>
- Khalaj, O., Abedin Nejad, S., & Janda, T. (2021). Multi Elements Simulation of Biaxial Test with Two Different Soil Layers Using Hypoplastic Constitutive Model. *IOP Conference Series: Materials Science and Engineering*, 1161(1), 012001. <https://doi.org/10.1088/1757-899x/1161/1/012001>
- Kolymbas, D. (1991). An outline of hypoplasticity. *Archive of Applied Mechanics*, 61, 143–151.
- Mašín, D. (2015). The influence of experimental and sampling uncertainties on the probability of unsatisfactory performance in geotechnical applications. *Geotechnique*, 65(11), 897–910. <https://doi.org/10.1680/jgeot.14.P.161>
- Mašín, D. (2019). *Modelling of Soil Behaviour with Hypoplasticity: Another Approach to Soil Constitutive Modelling*.
- Mohammadi-Haji, B., & Ardakani, A. (2020). Calibration of a Hypoplastic Constitutive Model with Elastic Strain Range for Firoozkuh Sand. *Geotechnical and Geological Engineering*, 38(5), 5279–5293. <https://doi.org/10.1007/s10706-020-01363-w>
- Moussa, A., Salah, M., & Rafik, D. (2020). Improvement of a Hypoplastic Model for Granular Materials Under High-Confining Pressures. *Geotechnical and Geological Engineering*, 38(4), 3761–3771. <https://doi.org/10.1007/s10706-020-01256-y>
- Namaei-kohal, A., Ardakani, A., & Hassanlourad, M. (2022). Hypoplastic soil model parameters calibration for Tehran silica sand and verification with a monotonic geocell pullout test. *Arabian Journal of Geosciences*, 15(9). <https://doi.org/10.1007/s12517-022-10110-9>
- Ng, C. W. W., Boonyarak, T., & Mašín, D. (2013). Three-dimensional centrifuge and numerical modeling of the interaction between perpendicularly crossing tunnels. *Canadian Geotechnical Journal*, 50(9), 935–946. <https://doi.org/10.1139/cgj-2012-0445>
- Niemunis, A., & Herle, I. (1997). Hypoplastic model for cohesionless soils with elastic strain range. *Mechanics of Cohesive-Frictional Materials*, 2(4), 279–299. [https://doi.org/10.1002/\(SICI\)1099-1484\(199710\)2:4<279::AID-CFM29>3.0.CO;2-8](https://doi.org/10.1002/(SICI)1099-1484(199710)2:4<279::AID-CFM29>3.0.CO;2-8)
- Niemunis, A., Wichtmann, T., & Triantafyllidis, T. (2005). A high-cycle accumulation model for sand. *Computers and Geotechnics*, 32(4), 245–263. <https://doi.org/10.1016/j.compgeo.2005.03.002>
- Poblete, M., Fuentes, W., & Triantafyllidis, T. (2016). On the simulation of multidimensional cyclic loading with intergranular strain. *Acta Geotechnica*, 11(6), 1263–1285. <https://doi.org/10.1007/s11440-016-0492-2>
- Stutz, H. H., & Wuttke, F. (2018). Hypoplastic modeling of soil-structure interfaces in offshore applications. *Journal of Zhejiang University: Science A*, 19(8), 624–637. <https://doi.org/10.1631/jzus.A1700469>
- Stutz, H., Mašín, D., Sattari, A. S., & Wuttke, F. (2017). A general approach to model interfaces using existing soil constitutive models application to hypoplasticity. *Computers and Geotechnics*, 87, 115–127. <https://doi.org/10.1016/j.compgeo.2017.02.010>
- Stutz, H., Mašín, D., & Wuttke, F. (2016). Enhancement of a hypoplastic model for granular soil-structure interface behaviour. *Acta Geotechnica*, 11(6), 1249–1261. <https://doi.org/10.1007/s11440-016-0440-1>
- Tasan, H. E., & Yilmaz, S. A. (2019). Effects of installation on the cyclic axial behaviour of suction buckets in sandy soils. *Applied Ocean Research*, 91(August), 101905. <https://doi.org/10.1016/j.apor.2019.101905>
- Tsegaye, A. B., Molenkamp, F., Brinkgreve, R. B. J., Bonnier, P. G., De Jager, R., & Galavi, V. (2010). Modeling liquefaction behavior of sands by means of hypoplastic model. *Numerical Methods in Geotechnical Engineering - Proceedings of the 7th European Conference on Numerical Methods in Geotechnical Engineering*, 1, 81–87. <https://doi.org/10.1201/b10551-18>
- von Wolffersdorff, P. A. (1996). Hypoplastic relation for granular materials with a predefined limit state surface. *Mechanics of Cohesive-Frictional Materials*, 1(3), 251–271. [https://doi.org/10.1002/\(SICI\)1099-1484\(199607\)1:3<251::AID-CFM13>3.0.CO;2-3](https://doi.org/10.1002/(SICI)1099-1484(199607)1:3<251::AID-CFM13>3.0.CO;2-3)
- Wichtmann, T., Fuentes, W., & Triantafyllidis, T. (2019). Inspection of three sophisticated constitutive models based on monotonic and cyclic tests on fine sand: Hypoplasticity vs. Sanisand vs. ISA. *Soil Dynamics and Earthquake Engineering*, 124(April 2018), 172–183. <https://doi.org/10.1016/j.soildyn.2019.05.001>
- Yang, Z., Liao, D., & Xu, T. (2020). A hypoplastic model for granular soils incorporating anisotropic critical state theory. *International Journal for Numerical and Analytical Methods in Geomechanics*, 44(6), 723–748. <https://doi.org/10.1002/nag.3025>